Supporting Information

Thrombin-Activatable Microbubbles as Potential Ultrasound Contrast Agents for the Detection of Acute Thrombosis

Jacques Lux[1], Alexander M. Vezeridis[2], Kenneth Hoyt[1,3], Stephen R. Adams[4], Amanda M. Armstrong[1], Shashank R. Sirsi[1,3], Robert F. Mattrey[1]**

[1] Department of Radiology, Translational Research in Ultrasound Theranostics (TRUST) Research Program, University of Texas Southwestern Medical Center, 5323 Harry Hines Blvd, Dallas, TX 75390-8514

[2] Department of Radiology, University of California , San Diego, La Jolla, CA 92093

[3] Erik Jonsson School of Engineering & Computer Science, University of Texas at Dallas, Richardson, TX 75080

[4] Department of Pharmacology, University of California, San Diego, La Jolla, CA 92093, USA

Corresponding Authors

Prof. Jacques Lux, E-mail address: Jacques.Lux@UTSouthwestern.edu

Prof. Robert F. Mattrey, E-mail address: Robert.Mattrey@UTSouthwestern.edu

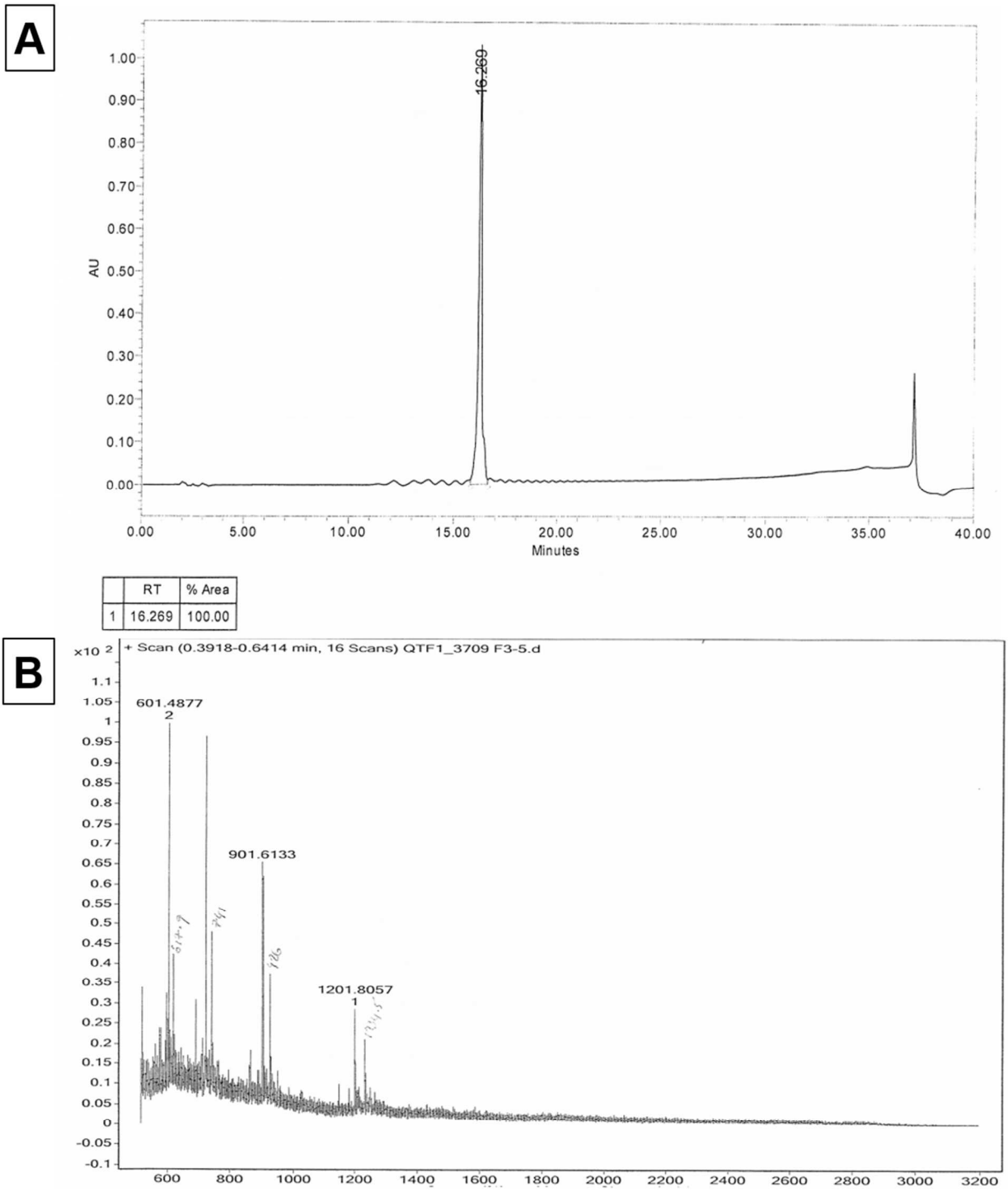

Figure S1. Characterization of ACPP. A) HPLC chromatogram and B) ES-MS spectrum showing the fragments of ACPP (m/z: 1201.8057 (z = 3), 901.6133 (z = 4), 601.4877 (z = 6)).

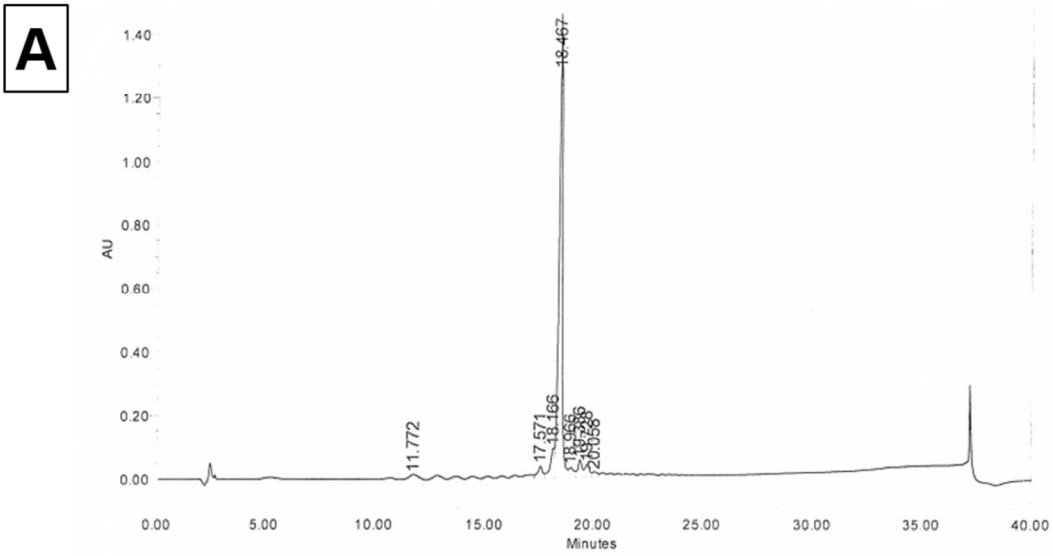

	RT	% Area
1	11.772	2.11
2	17.571	2.91
3	18.166	5.87
4	18.467	78.41
5	18.966	2.72
6	19.386	3.74

	RT	% Area
7	19.728	2.96
8	20.058	1.28

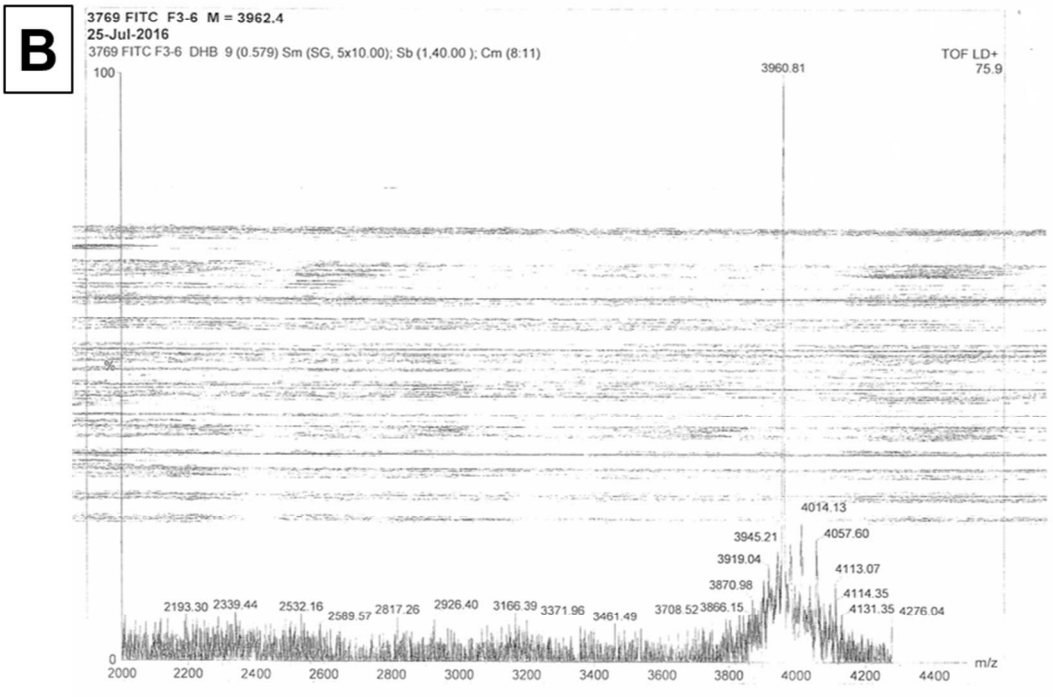

Figure S2. Characterization of FITC-ACPP. A) HPLC chromatogram and B) MALDI-TOF spectrum showing the mass of FITC-ACPP: 3960.81 Da, (calculated 3962.4 Da).

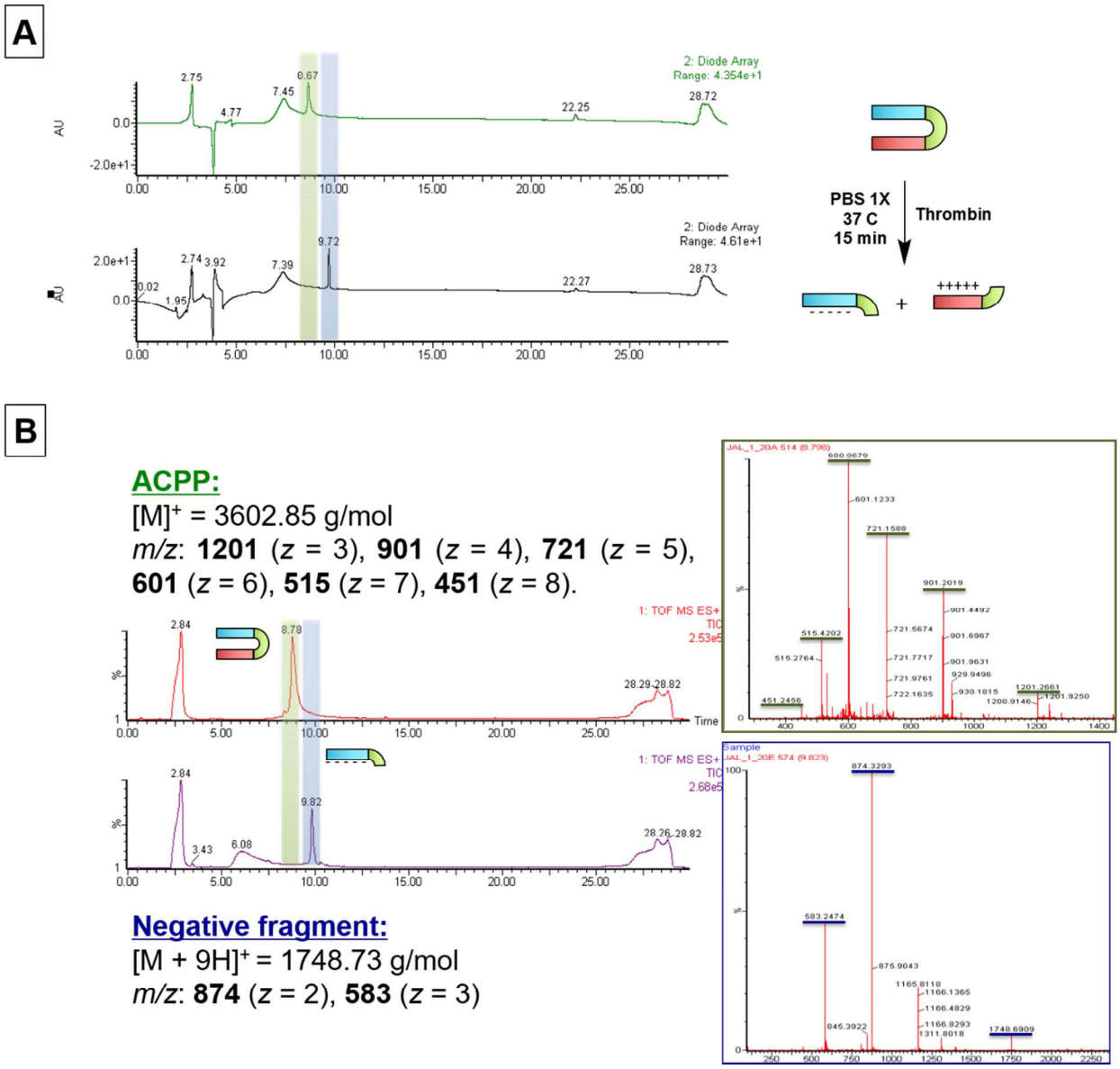

Figure S3. Confirmation by LC-MS of thrombin-directed cleavage of ACPP. A) HPLC Chromatograms (Diode array-UV channel) of ACPP before (top) and after (bottom) cleavage by thrombin. B) ES-MS spectrum of ACPP before (top) and after (bottom) cleavage by thrombin. Mass fragments for ACPP were identified (*m/z*: 1201.2661 (z = 3), 901.2019 (z = 4), 721.1588 (z = 5), 601.1233 (z = 6), 515.2764 (z = 7), 451.2456 (z = 8)). Masses of the polyanionic inhibitory domain and its fragments were identified: 1748.6909 Da, (calculated $[M + 9H]^{+}$ = 1748.73 Da). *m/z*: 874.3293 (z = 2), 583.2474 (z = 3).

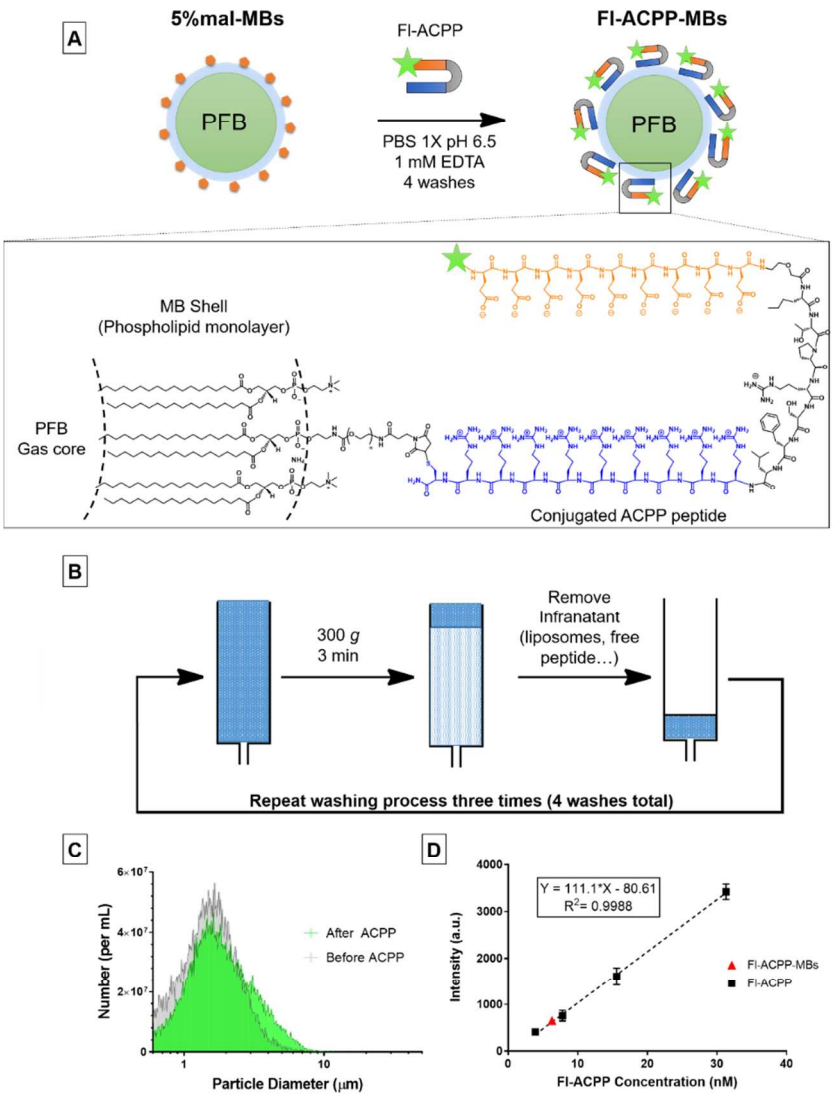

Figure S4. A) Schematic representation of Fl-ACPP conjugation on maleimide-bearing microbubbles. B) Schematic representation of the washing process of the microbubbles with first a low speed centrifugation to make buoyant rise in the syringe followed by the removal of the infranatant containing liposomes or free peptide. The process was repeated 3 times for a total of 4 washes. C) Microbubbles concentrations and size distributions measured with multisizer before Fl-ACPP conjugation (grey) and after Fl-ACPP conjugation (green). D) Fluorescence spectroscopy calibration curve of Fl-ACPP and data point for Fl-ACPP-MBs (1:400 dilution), N=4.

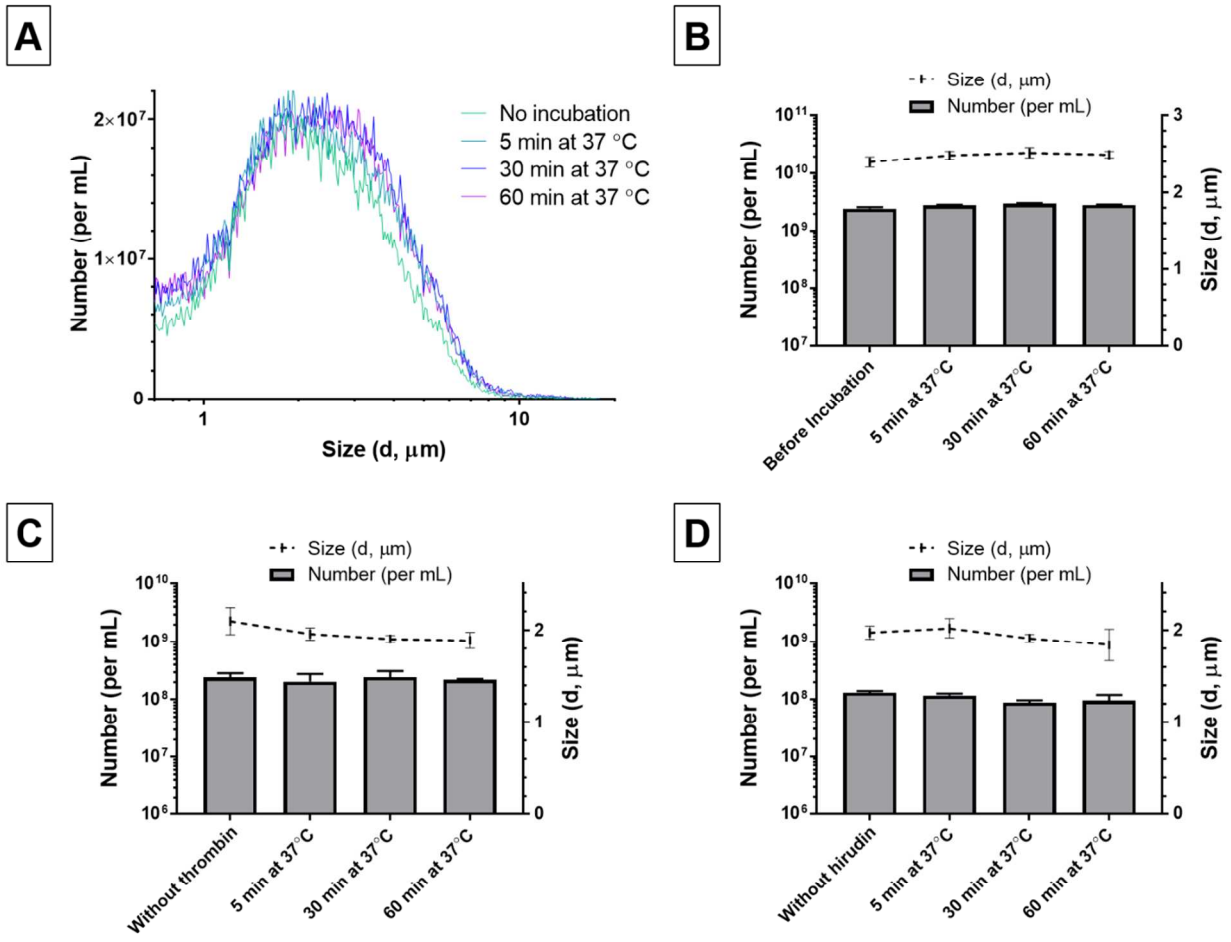

Figure S5. Stability of ACPP-MBs over time at 37 ˚C. A) ACPP-MBs size distributions measured with multisizer before and after 5, 30 and 60 minutes of incubation at 37 ˚C. B) Size (d, µm) and concentration (MBs/mL) of ACPP-MBs before and after 5, 30 and 60 minutes of incubation at 37 ˚C. C) Size (d, µm) and concentration (MBs/mL) of ACPP-MBs before and after 5, 30 and 60 minutes of incubation in the presence of 280 nM thrombin at 37 ˚C. D) Size (d, µm) and concentration (MBs/mL) of ACPP-MBs before and after 5, 30 and 60 minutes of incubation with hirudin at 37 ˚C.

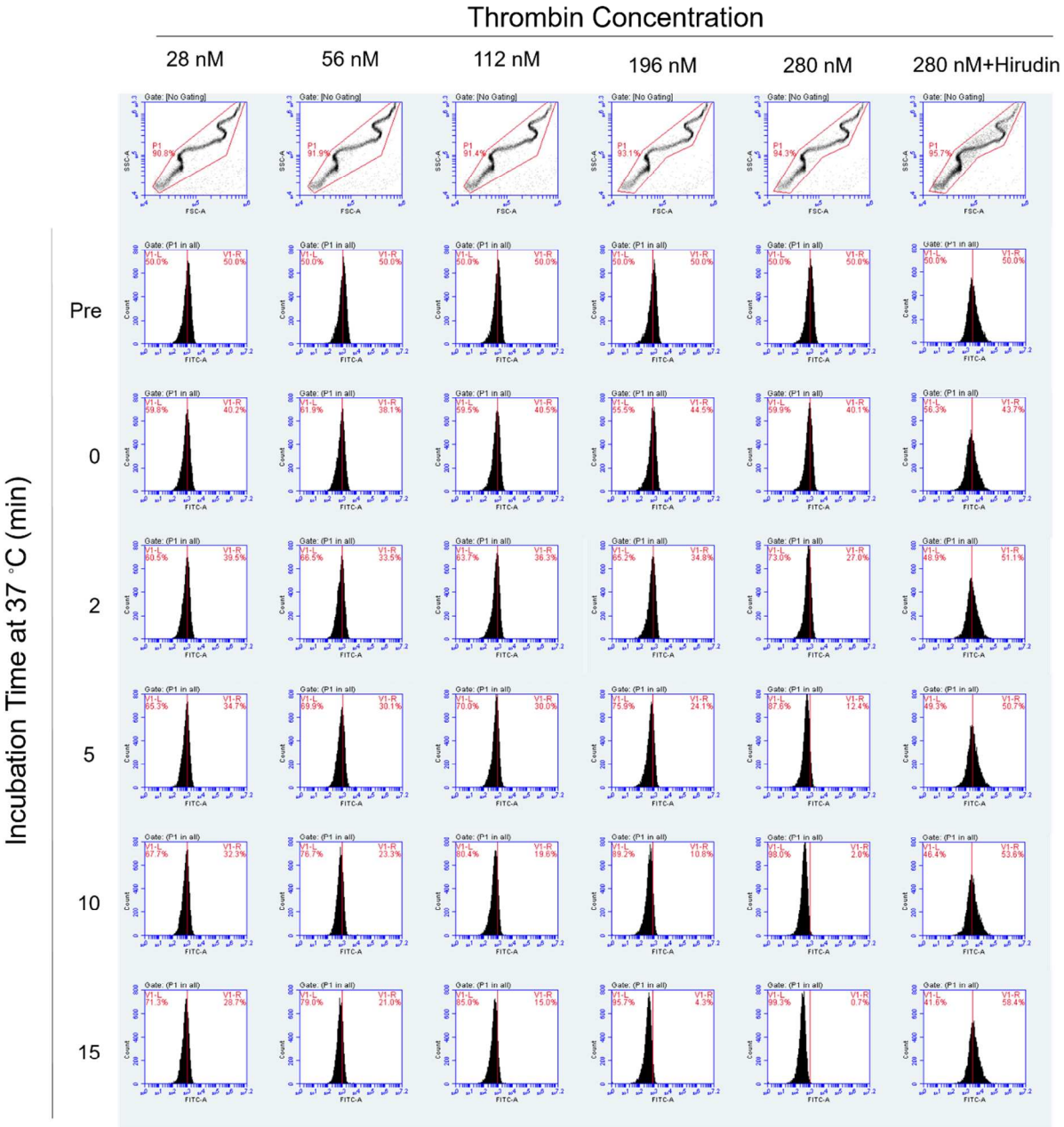

Figure S6. Study of ACPP-MBs cleavage kinetics with flow cytometry. The region on the scatter plot (first row) corresponding to the MBs was identified and the fluorescence signal was gated to provide the mean fluorescence intensity after incubation with increasing thrombin concentrations at different incubation times from before to 15 minutes at 37 °C .

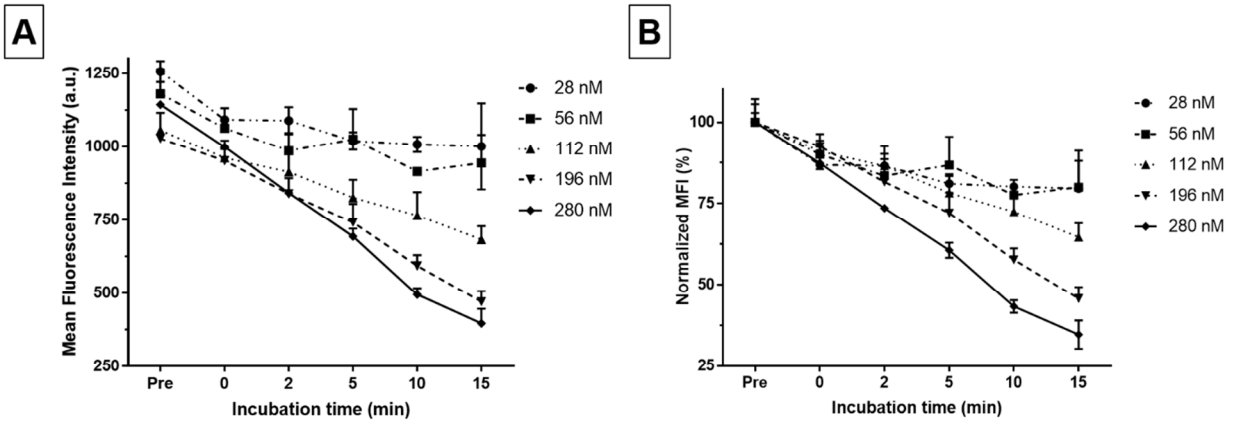

Figure S7. Mean Fluorescence Intensity (MFI) of FITC-ACPP-MBs measured by flow cytometry before and after cleavage with thrombin. A) MFI of FITC-ACPP-MBs before and after incubation with thrombin at concentrations of 28, 56, 112, 196 and 280 nM. B) Normalized MFI of FITC-ACPP-MBs before and after incubation with thrombin at concentrations of 28, 56, 112, 196 and 280 nM.

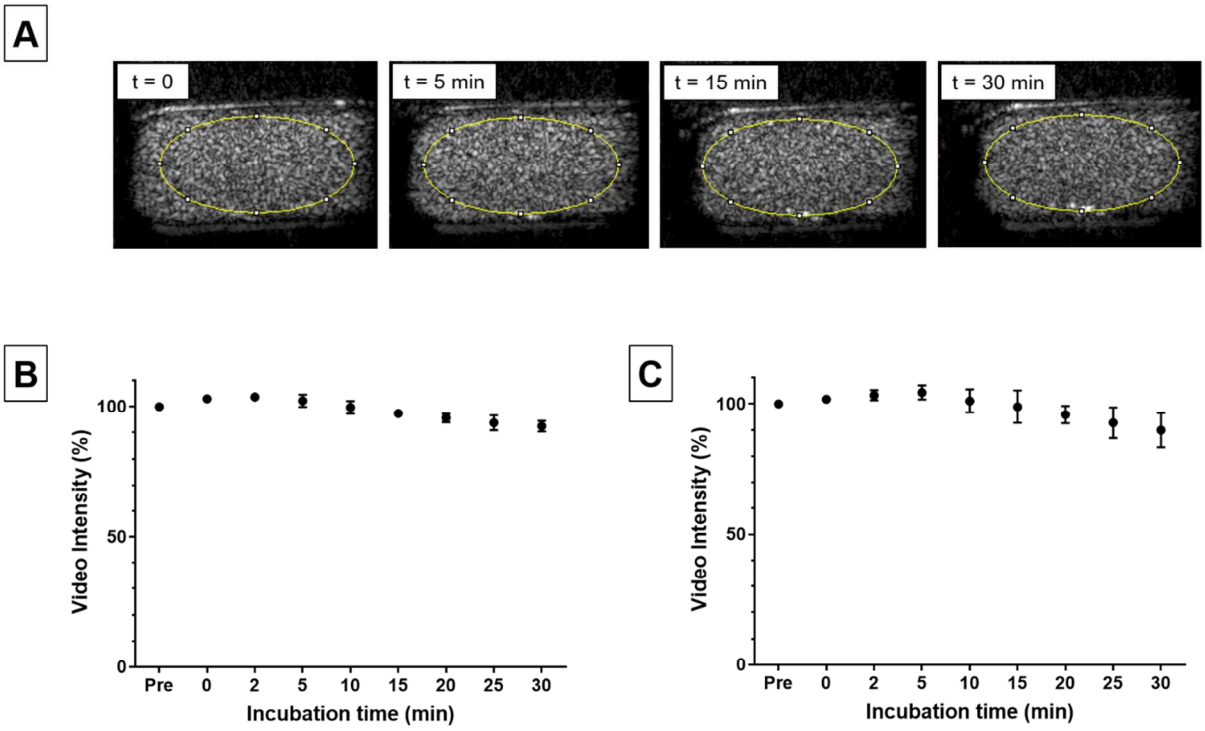

Figure S8. Ultrasound video intensity of ACPP-MBs over time at 37 °C. A) Representative greyscale US images of ACPP-MBs incubated at 37 °C in the presence of thrombin or hirudin. B) Normalized video intensity of ACPP-MBs before addition of thrombin and after incubation with thrombin at 37 °C over 30 minutes. C) Normalized video intensity of ACPP-MBs before addition of hirudin and after incubation with thrombin at 37 °C over 30 minutes.

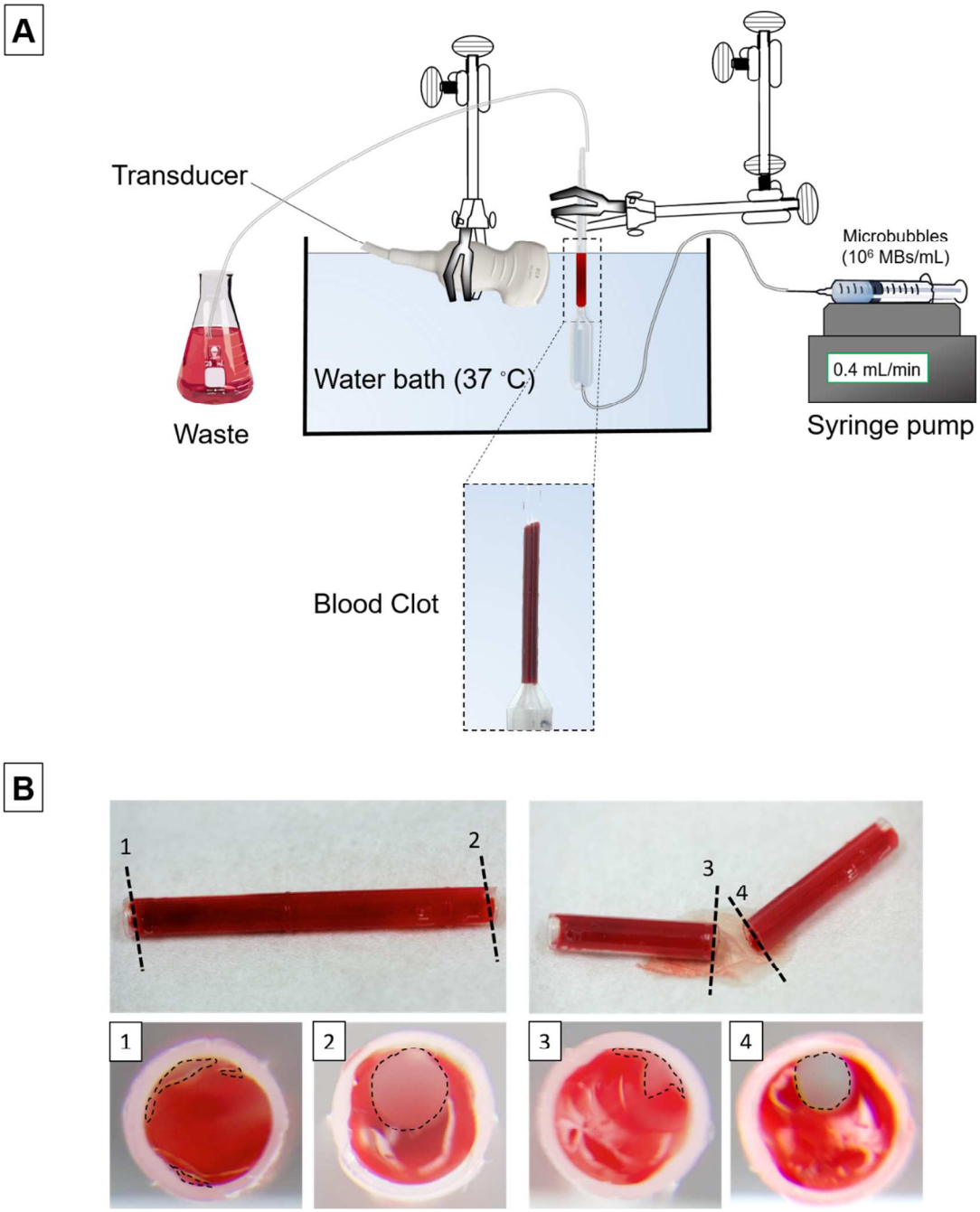

Figure S9. Experimental setup for in vitro ultrasound imaging. A) Schematic representation of the in vitro experimental setup for the ultrasound imaging of clots with ACPP-MBs, MBs or ACPP-MBs + hirudin (inset: photograph of a clot prepared for one of the experiments). B) Representative photographs of cross sections of the clot taken at both ends (1 & 2) and at the

center (3 & 4) showing the presence of channels (black dotted line) that allow passage of MBs through the clot.

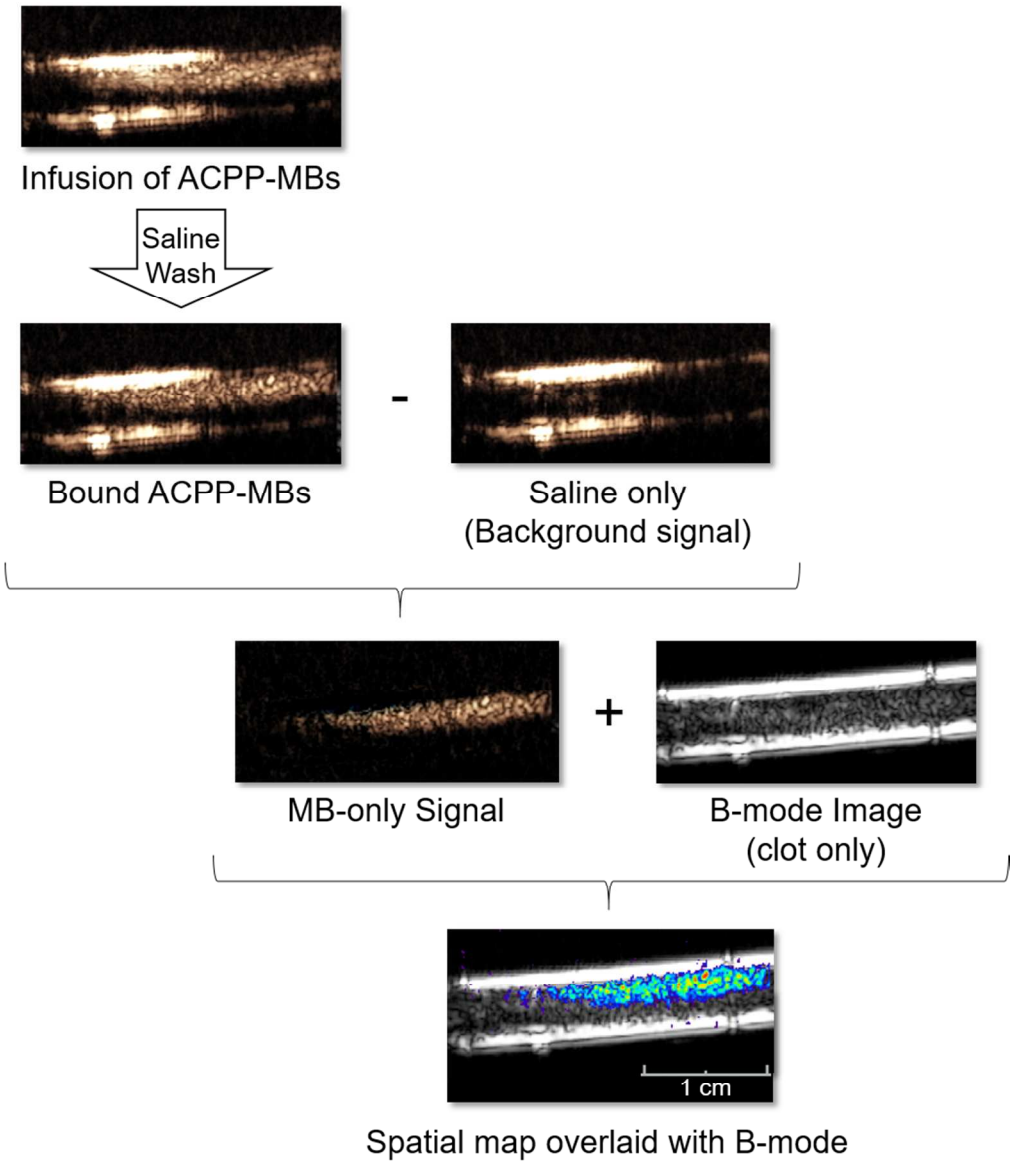

Figure S10. CPS images of the clot during diffusion, after saline wash with or without ACPP-MBs. MB-only signal was obtained by subtraction of bound MB signal by saline only signal (background) through the clot. The obtained signal was overlaid with the B-mode image of the clot to yield the spatial map represented in Figure 6.

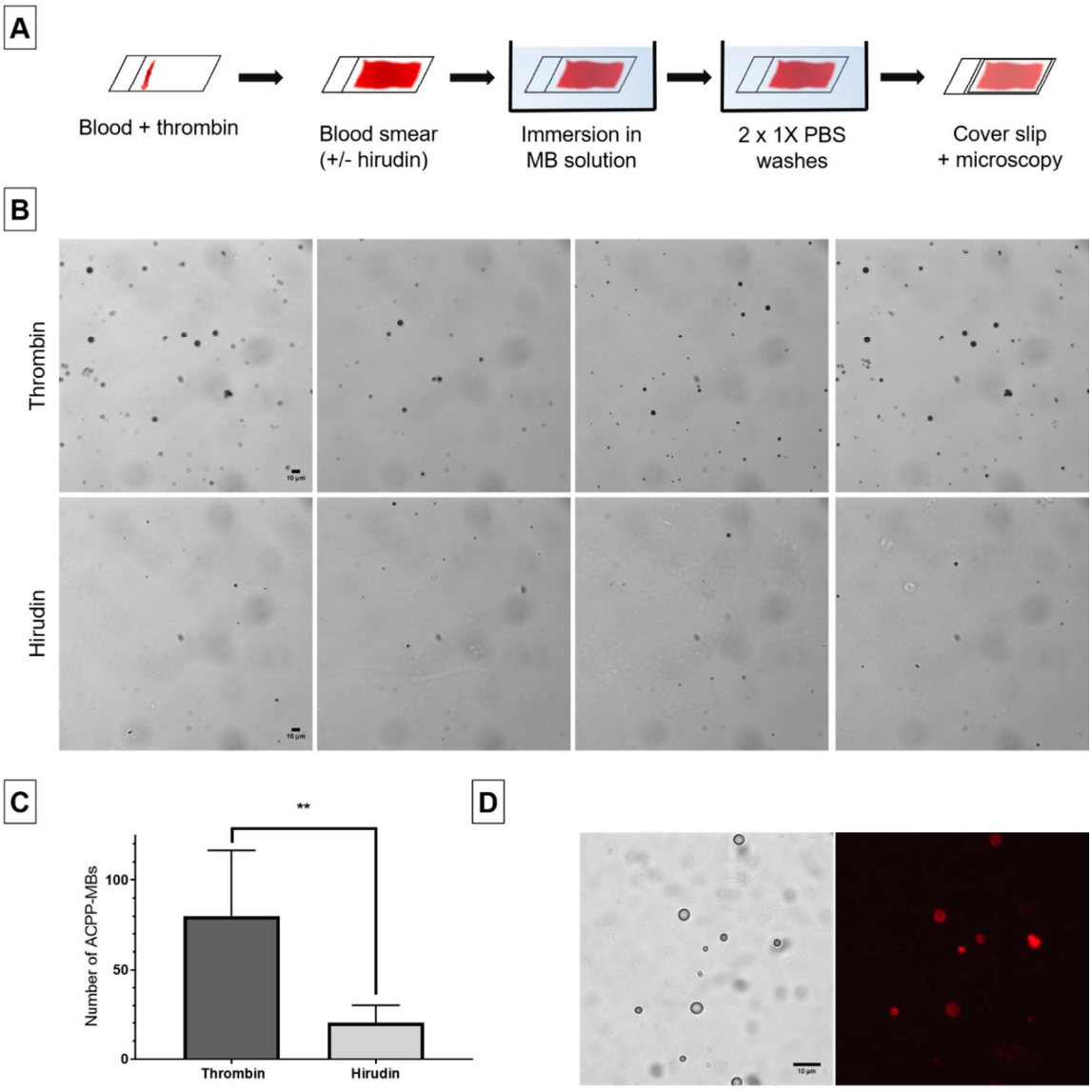

Figure S11. Optical imaging of ACPP-MBs on a blood smear. A) Schematic representation of the experimental procedure. B) Representative images of bound ACPP-MBs on blood smear with active thrombin (top) and with thrombin inhibited with hirudin (bottom). C) Number of microbubbles visible per field of view at 20X magnification (N = 7). Scale bar = 10 µm. D) Bright field (left) and fluorescence (right) images at 63X magnification of DiD-labeled ACPP-MBs bound to the blood smear. Scale bar = 10 µm. Error bars represent Standard Deviation. ** $p < 0.01$.